A method to compute the local birefringence vector in twisted and bent antiresonant hollow-core fibers

Gianluca Guerra,[1,*] Seyed Mohammad Abokhamis Mousavi,[1] Austin Taranta,[1] Eric Numkam Fokoua,[1] Marco Santagiustina,[2] Andrea Galtarossa,[2] Francesco Poletti,[1] and Luca Palmieri[2]

[1] *Optoelectronics Research Centre, University of Southampton, Southampton, SO17 1BJ, United Kingdom*
[2] *Department of Information Engineering, University of Padova, 35131, Padova, Italy*
[*] *g.guerra@soton.ac.uk*

Abstract: This work proposes a technique to elucidate mode coupling when antiresonant fibers are twisted and bent. From this, we show how the birefringence of a nested antiresonant nodeless fiber changes as function of the deployment.

1. Introduction

Antiresonant hollow-core fibers (ARFs) [1] have attracted the interest of the optical community because they can bring the advantages of free space propagation to the world of fiber optics. The promise of low non-linearity, whopping available bandwidth, and exceptional polarization purity has driven research to reduce attenuation in these structures [2]. Nested antiresonant nodeless fibers (NANFs) and double nested antiresonant fibers (DNANFs) [3] have now achieved a loss comparable to solid-core fibers, so they are legitimate candidates for deployment in real-world applications, from telecommunications to optical sensors. It is thus of paramount importance to be able to model and predict the fiber performance under different deployment conditions.

The techniques used to model the performance depend on the problem at hand. When an ARF is uniform along its length, its performance is determined by the modes supported by its cross-section. In this case, one can employ the finite element method (FEM) or other numerical methods to solve for the modes. In all the other cases though, modes do not exist strictly, and one should employ analyses based on coupled-mode theories (CMTs), where the modes of the uniform straight fiber are used to expand the electromagnetic field of non-uniformly deployed fibers. This technique is rarely used in ARFs because CMTs fail to treat geometrical deformation rigorously and cannot work with highly lossy modes. To address these shortfalls, we recently developed a more general approach—the *unified coupled-mode theory* (UCMT) [4]—which is well suited for ARFs. Here, we use it to analyse the polarization properties of a 5-tube NANF deployed under bend and twist, conditions similar to those that the fiber would encounter if coiled.

The polarization properties of an ARF are determined by its fundamental mode (FM). Indeed, the fiber guiding mechanism strips high-order modes (HOMs) out from the core, making the fiber virtually single mode after sufficient propagation length. This single mode approximation is so effective that HOMs are rarely considered in practice; nevertheless, they remain legitimate electromagnetic solutions that might couple with the FM, so they must be included in the CMT. Actually, a reliable description of ARFs in terms of CMT requires hundreds of modes, preventing researchers from having a clear physical understanding of the fiber polarization properties in terms of familiar quantities such as the birefringence vector. We show here a numerical method to reduce the coupled-mode equation from an $N \times N$ system that encloses the coupling information, where N is the number (in the order of a few hundreds) of considered modes, to a 2×2 system that distills the fiber local polarization properties. We apply the method to the twisted and bent 5-tube NANF, and we extract its local birefringence vector from the reduced system. This method can be used any time the deployed ARF remains virtually single mode.

2. Theoretical model

When the fiber is deployed in a coil, it is subject to a complex combination of twist and bend. In this preliminary work, we consider a simpler case where the plane of the bend, the bending radius R_b, and the twist rate $\dot{\tau}$ are all constants. In these settings, the coordinate deformation that twists and bends a straight fiber is $x(u,v,s) = -R_b + [R_b + u\cos\tau(s) + v\sin\tau(s)]\cos(s/R_b)$, $y(u,v,s) = v\cos\tau(s) - u\sin\tau(s)$, and $z(u,v,s) = [R_b + u\cos\tau(s) + v\sin\tau(s)]\sin(s/R_b)$, where (u,v,s) is the local Cartesian coordinate system centered at the fiber, and (x,y,z) is the laboratory Cartesian coordinate system of the deployed fiber. As it is defined, $\tau(s)$ is the angle that the cross-section has rotated because of twist, namely $\tau(s) = \dot{\tau}s$. Since we are considering ARFs, most of the

light is confined in the hollow-core; therefore, the stress-induced effects occurring in the glass when the fiber is deployed are negligible.

A fiber deployed in this configuration can be studied by using the UCMT. The theory first exploits transformation optics (TO) to define a waveguide electromagnetically equivalent to the deployed fiber, then it describes the propagation in terms of the equivalent waveguide and the modes of the straight fiber—we refer the reader to the original paper for a detailed explanation [4]. The propagation within the equivalent waveguide is described, in terms of the modes of the straight fiber, by the coupled-mode equation $\mathrm{d}\mathbf{a}/\mathrm{d}s = -j\left[\mathbf{D}+\mathbf{X}(s)\right]\mathbf{a}(s)$, where $\mathbf{a}$ is the vector of the complex amplitudes of the modes, $\mathbf{D}$ is the diagonal matrix of the mode propagation constants, and $\mathbf{X}$ is the coupling matrix. Although the twist rate and bending radius are constant, the coupling matrix still depends on the coordinate s because the fiber cross-section bends towards different orientations as is rotated by the twist. Therefore, one must compute $\mathbf{X}$ at each cross-section rotation $\tau(s)$. This is computationally expensive since each $\mathbf{X}$ is derived from the evaluation of N^2 overlap integrals. However, a closer look at the overlap integral reveals that $\mathbf{X}$ is a linear combination of three coupling matrices:

$$\mathbf{X}(\tau(s)) = \dot{\tau}\,\bar{\mathbf{X}}_{\text{twist}} + \left(\bar{\mathbf{X}}_{\text{bend}}(0)\cos\tau(s) + \bar{\mathbf{X}}_{\text{bend}}(\pi/2)\sin\tau(s)\right)/R_b, \tag{1}$$

where $\bar{\mathbf{X}}_{\text{twist}}$ is the coupling matrix obtained by twisting the fiber with $\dot{\tau} = 1\,\text{rad/m}$, and $\bar{\mathbf{X}}_{\text{bend}}(0)$ and $\bar{\mathbf{X}}_{\text{bend}}(\pi/2)$ are those obtained by bending the fiber with $R_b = 1\,\text{m}$ when the cross-section has rotated by 0 and $\pi/2$ radians, respectively. Eq. (1) provides a method to compute the coupling matrix at any $\tau(s)$, R_b, and $\dot{\tau}$ values, at the cost of computing only three coupling matrices.

The coupled-mode equation contains all the information about the propagation, which can be numerically solved to find the fiber polarization properties, yet the inspection of the coupling matrix does not provide any physical insights. Indeed, when the fiber is twisted and bent, the FM couples strongly with the HOMs in the equivalent waveguide, forming an intricate relation of direct and indirect coupling from which the FM is hard to disentangle. This seems counter-intuitive when examining ARFs which are virtually single mode. In reality, the single mode approximation is recovered by changing the basis of the modes used in the UCMT, from the modes of the straight fiber to the *local* modes of the equivalent waveguide. The local modes can be found by diagonalizing matrix $\mathbf{D}+\mathbf{X}(\tau(s))$: their propagation constants are the eigenvalues; and their fields, expressed in the basis of the modes of the straight fiber, are the eigenvectors. If we call $\mathbf{\Lambda}(\tau(s))$ the diagonal matrix of the eigenvalues and $\mathbf{V}(\tau(s))$ the matrix of the eigenvectors, we can write the coupled-mode equation concerning the amplitudes $\mathbf{b}(s) = \mathbf{V}^{-1}(\tau(s))\,\mathbf{a}(s)$ of the local modes as $\mathrm{d}\mathbf{b}/\mathrm{d}s = -j\mathbf{N}(\tau(s))\,\mathbf{b}(s)$ with $\mathbf{N} = \mathbf{\Lambda} - j\dot{\tau}\mathbf{V}^{-1}\,(\mathrm{d}\mathbf{V}/\mathrm{d}\tau)$. Matrix $\mathbf{N}$ is nearly block diagonal, with a 2×2 block $\mathbf{N}_2$ that regards the local FM. Therefore, a reduced coupled-mode equation for the local FM can be obtained as $\mathrm{d}\mathbf{b}_2/\mathrm{d}s = -j\mathbf{N}_2(\tau(s))\,\mathbf{b}_2(s)$, where $\mathbf{b}_2$ is the vector of the local FM amplitudes. Considering this reduced system, we go back to the basis of the FM of the straight fiber by using the change of basis $\mathbf{a}_2(s) = \mathbf{V}_2(\tau(s))\,\mathbf{b}_2(s)$, where $\mathbf{V}_2$ is the reduced matrix $\mathbf{V}$. In the basis of the FM, the coupled-mode equation is $\mathrm{d}\mathbf{a}_2/\mathrm{d}s = -j\mathbf{L}_2(\tau(s))\,\mathbf{a}_2(s)$, where $\mathbf{L}_2 = \mathbf{V}_2\mathbf{N}_2\mathbf{V}_2^{-1} + j\dot{\tau}\,(\mathrm{d}\mathbf{V}_2/\mathrm{d}\tau)\,\mathbf{V}_2$. Finally, we use TO to relate the amplitudes of the FM in the equivalent waveguide to those in the twisted and bent fiber. In particular, it can be shown that the latter are related to the former as $\tilde{\mathbf{a}}_2(s) = \mathbf{R}_2^{\top}(\tau(s))\,\mathbf{a}_2(s)$, where $\mathbf{R}_2$ is the standard, two dimensional, rotation matrix. Accordingly, the equation that describes the evolution of the amplitudes $\tilde{\mathbf{a}}_2$ is $\mathrm{d}\tilde{\mathbf{a}}_2/\mathrm{d}s = -j\tilde{\mathbf{L}}_2(\tau(s))\,\tilde{\mathbf{a}}_2(s)$, where $\tilde{\mathbf{L}}_2 = \mathbf{R}_2^{\top}\mathbf{L}_2\mathbf{R}_2 - j\dot{\tau}\mathbf{R}_2^{\top}\,(\mathrm{d}\mathbf{R}_2/\mathrm{d}\tau)$. Matrix $\tilde{\mathbf{L}}_2$ is the 2×2 complex matrix that describes the propagation of the FM within the twisted and bent fiber. The FM has degenerate polarization modes and thus, we only require $\tilde{\mathbf{L}}_2$ to yield exhaustive information about the local polarization properties of the fiber, and the integration of $-j\tilde{\mathbf{L}}_2$ along s yields its Jones matrix. Moreover, as in standard solid-core single mode fibers, $\tilde{\mathbf{L}}_2$ can be translated to the 3-dimensional vector $\boldsymbol{\kappa}$ in the Stokes space, whose components are $\kappa_i = \mathrm{tr}(\tilde{\mathbf{L}}_2\,\boldsymbol{\sigma}_i)/2$, where $\boldsymbol{\sigma}_i$ is the i-th Pauli's matrix. One can obtain the local birefringence vector $\boldsymbol{\beta}$ and local dichroism vector $\boldsymbol{\alpha}$ (if non-negligible) as twice the real and imaginary part of $\boldsymbol{\kappa}$, respectively [5]. These two vectors give complete and intuitive information about the polarization behavior of the fiber.

3. Results

To demonstrate the power of this method, we study the polarization properties of a twisted and bent 5-tube NANF. We show that, concerning the FM, the reduced 2×2 system is a close approximation of the full system. As a result, the information about the local birefringence and dichroism vectors can be extracted from the model. We discuss the properties of local birefringence vector as an example.

We assume the 5-tube NANF to have symmetric cross-section and to be deployed with different configurations of bend and twist. We vary the bending radius from 2.5 cm to 10 cm and the twist rate from 0.1 rad/m to 10 rad/m; each combination of bend and twist is considered constant along the fiber. At each configuration, we first compute the coupling matrix $\mathbf{X}(\tau(s))$ as per Eq. (1), where 380 modes of the straight fiber are used to compute the matrices $\bar{\mathbf{X}}_{\text{twist}}$, $\bar{\mathbf{X}}_{\text{bend}}(0)$, and $\bar{\mathbf{X}}_{\text{bend}}(\pi/2)$. Then, we reduce the coupled-mode equation from 380×380 to 2×2 by following the technique introduced in the previous section, obtaining $\tilde{\mathbf{L}}_2(\tau(s))$.

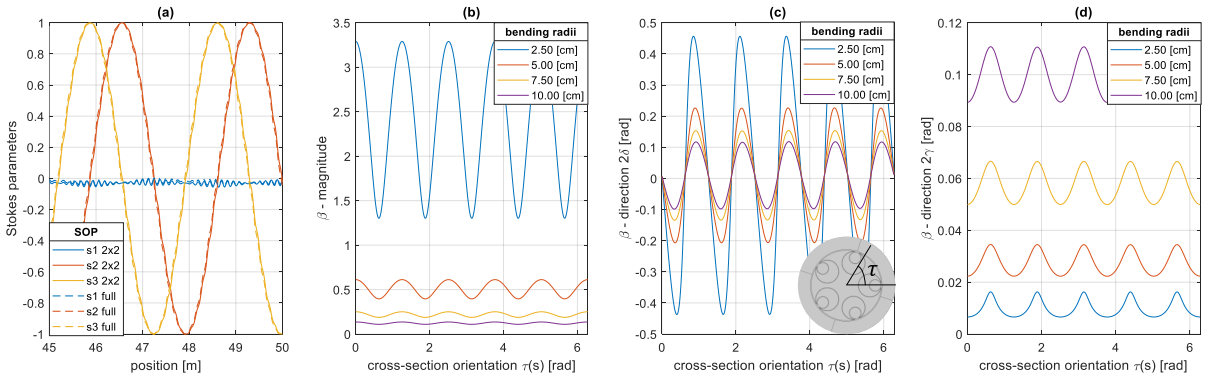

Fig. 1. (a) SOP evolution; (b) magnitude, (c) direction angle 2δ, and (d) direction angle 2γ of the local birefringence vector. Inset: 5-tube NANF cross-section.

To validate the reduction technique, we compare the state of polarization (SOP) obtained by integrating $-j\tilde{\mathbf{L}}_2$ over s to that obtained by propagating the full coupled-mode 380-dimensional system. Fig. 1(a) shows the evolution of the SOP of the last 5 m piece of the 50 m long 5-tube NANF, twisted with $\dot{\tau} = 10$ rad/m and bent with $R_b = 2.5$ cm, where we launched a $+45°$ linear SOP at the fiber input. Results show an excellent agreement between the SOP obtained from the 2×2 $\tilde{\mathbf{L}}_2$ matrix and that obtained from the full $\mathbf{D}+\mathbf{X}$ matrix; agreement is also achieved at all the other configurations of twist and bend.

We compute the local birefringence vector $\boldsymbol{\beta}$ as explained in the theoretical model, and we represent it against $\tau(s)$, at different values of R_b, in terms of its magnitude and direction. We express the vector direction as 2δ and 2γ, where 2δ is the angle that $\boldsymbol{\beta}$ forms with the vector (1, 0, 0) when projected in the $s_1 - s_2$ plane in the Stokes space (i.e., the linearity), and 2γ is the angle that defines the circular component of the birefringence as $\beta_3 = |\boldsymbol{\beta}|\sin(2\gamma)$. Fig. 1(b) shows that the magnitude of the birefringence vector at $\dot{\tau} = 10$ rad/m. The magnitude is a periodic function of $\tau(s)$ with period $2\pi/5$, which is clearly related to the number of tubes. It can be shown that the birefringence is maximum when the bend squeezes the field towards a tube and is minimum when the bend is towards a gap between tubes. Predictably, the birefringence increases with the decreasing of R_b. Like the magnitude, the direction of the birefringence vector is periodic with period $2\pi/5$. Fig. 1(c) and Fig. 1(d) show the angles 2δ and 2γ obtained at $\dot{\tau} = 10$ rad/m. The angle 2δ oscillates around zero, which corresponds to the direction parallel to that of the bending when observed from the laboratory frame. For bending directly toward a tube or a gap, the structural features are balanced about the bend, and the birefringence vector coincides exactly with the bend direction. For other bend directions, the birefringence vector tends to orient toward the tube centered nearest to the bend direction. As R_b decreases, this deviation between birefringence vector orientation and bend direction becomes increasingly marked. The angle 2γ sets the amount of circular birefringence: since it is not zero, there is a (small) amount of circular birefringence. As 2γ decreases with the decreasing of the bending radius, linear birefringence is the dominant effect at tight bends.

The periodic behavior of the magnitude and direction of the birefringence vector is fundamentally different from what happens in standard single mode fibers, where the magnitude of the birefringence is decoupled from $\tau(s)$ and its direction is always aligned with the bending direction. This complex dynamic may produce polarization effects not seen in single mode fibers yet, and deserves future investigations.

This project acknowledges funding from Honeywell Inc. and the U.S. Government under the DoD Ordnance Technology Consortium (DOTC) Other Transaction Agreement (OTA) (W15QKN-18-9-1008); and support from the Italian Ministry of Research (law 232/2016; PRIN 2017, project FIRST).

References

1. N. M. Litchinitser, A. K. Abeeluck, C. Headley, and B. J. Eggleton, "Antiresonant reflecting photonic crystal optical waveguides," Opt. Lett., vol. 27, no. 18, pp. 1592–1594, Sep. 2002.
2. A. Taranta et al., "Exceptional polarization purity in antiresonant hollow-core optical fibres," Nat. Photon, vol. 14, no. 8, Aug. 2020.
3. G. T. Jasion et al., "0.174 dB/km Hollow Core Double Nested Antiresonant Nodeless Fiber (DNANF)," in 2022 Optical Fiber Communications Conference and Exhibition (OFC), Mar. 2022.
4. G. Guerra et al., "Unified Coupled-Mode Theory for Geometric and Material Perturbations in Optical Waveguides," J. Light. Technol., vol. 40, no. 14, pp. 4714–4727, Jul. 2022.
5. A. Galtarossa and L. Palmieri, "Theoretical analysis of reflectometric measurements in optical fiber links affected by polarization-dependent loss," J. Light. Technol., vol. 21, no. 5, pp. 1233–1241, May 2003.